



Published in final edited form as:

Anal Chem. 2001 September 01; 73(17): 4277–4285. doi:10.1021/ac0101050.

Long-Wavelength Long-Lifetime Luminophores

Badri P. Maliwal, Zgyunt Gryczynski, Joseph R. Lakowicz

Center for Fluorescence Spectroscopy, Department of Biochemistry and Molecular Biology, University of Maryland at Baltimore, 725 West Lombard Street, Baltimore, Maryland 21201

Abstract

We describe a new approach to making luminophores that display long emission wavelengths, long decay times, and high quantum yields. These luminophores are covalently linked pairs with a long-lifetime resonance-energy-transfer (RET) donor and a long-wavelength acceptor. The donor was a ruthenium (Ru) metal–ligand complex. The acceptor was the Texas Red. The donor and acceptor were covalently linked by polyproline spacers. The long-lifetime donor results in a long-lived component in the acceptor decay, which is due to RET. Importantly, the quantum yield of the luminophores approaches that of the higher quantum yield acceptor, rather than the lower quantum yield typical of metal–ligand complexes. The emission maxima and decay time of such tandem luminophores can be readily adjusted by selection of the donor, acceptor, and distance between them. Luminophores with these useful spectral properties can also be donor–acceptor pairs brought into close proximity by some biochemical association reaction. Luminophores with long-wavelength emission and long lifetimes can have numerous applications in biophysics, clinical diagnostics, DNA analysis, and drug discovery.

In fluorescence spectroscopy, the information available from an experiment is largely determined by the spectral properties of the fluorophore. For example, the anisotropy decay of fluorophores that display nanosecond decay times can be used to measure motions on the nanosecond time scale. If slower motions on the microsecond time scale are of interest, then it is necessary to use fluorophores that display microsecond decay times. Furthermore, intracellular fluorophores that require UV excitation result in a background of undesired emission due to the intrinsic fluorescence of cells and tissues. This autofluorescence from biological samples is mostly on the nanosecond time scale, and its intensity decreases at longer excitation and emission wavelengths. For these reasons, there is a need for fluorophores that display both long emission wavelengths and long decay times. To our knowledge, there are no luminophores that display the desired spectral properties of long decay times, long excitation and emission wavelengths, and high quantum yields.

During the past decade, a good number of fluorophores that display red or near-infrared (NIR) emission^{1–2} have become available. Such probes are widely used in the biochemical and medical applications of fluorescence, including protein labeling, DNA sequencing,^{3–9} and in vivo measurements.^{10–13} Many of the red/near infrared (NIR) fluorophores display high extinction coefficients and good quantum yields, both of which indicate the absorption and emission electronic transitions are strongly allowed. Consequently, the decay times of the red/NIR probes are typically under 2 ns, as is predicted by theory.¹⁴ The longest lifetime for red/NIR fluorophores is under 5 ns, which is found for some phthalocyanines and similar

structures.^{15–17} We are not aware of any approach to increasing the decay times without the use of an alternative process, such as phosphorescence.

We now describe a new approach to creating red/NIR luminophores that display both long decay times and high quantum yields. This approach is illustrated by the tandem luminophore in Scheme 1. This luminophore is based on resonance energy transfer (RET) from the ruthenium metal–ligand complexes (MLC) donor to the Texas Red (TR) acceptor. We use the term luminophore because emission from the MLCs displays both singlet and triplet character. We use a metal–ligand complex as the donor because the transition from the triplet excited state to the singlet ground state is not allowed, and these molecules display long lifetimes ranging from 100 ns to 10 μ s.^{18–20} Some MLCs that display still longer decay times from 50 to 260 μ s^{20–23} are known. Because of the long lifetimes, ease of synthesis, and range of spectral properties, the MLCs have been developed as luminescent probes in physical, analytical, and biophysical chemistry.^{24–31}

Although the MLCs display some favorable spectral properties, other properties are less favorable. The MLCs display low extinction coefficients, typically less than 20 000 M⁻¹ cm⁻¹, which is one reason for the long decay times,¹⁴ but which result in decreased sensitivity. Additionally, most MLCs display low quantum yields, which rarely exceed 0.1, and the quantum yields of the MLCs with the longest decay times are often smaller.^{20–23} Finally, the emission spectra are broad, which makes it more difficult to quantify the MLC emission in the presence of autofluorescence, because the background is also widely distributed across the wavelength scale.

In the present report, we describe a generic approach to overcoming these limitations of the available MLC and red/NIR probes, as typified in Scheme 1. The luminophore consists of a MLC, which displays a long lifetime, that is covalently linked to a high-quantum-yield acceptor. The luminophore is excited at a wavelength where the MLC absorbs, typically near 450 nm for the ruthenium (Ru) MLCs. The emission is red-shifted to longer wavelengths by RET to the red/NIR emitting acceptor. Some long wavelength probes have low absorption near 450 nm, so that most of the incident light is absorbed by the donor. Much, if not most, of the acceptor emission is, thus, due to energy transfer from the MLC. Following pulsed excitation, the excited state population of the MLC becomes the only excitation source for the acceptor, which continues to emit as long as MLCs remain in the excited state. Such luminophores can still display long decay times in the presence of RET. For instance, if the MLC donor displays a lifetime of 1 μ s in the absence of RET, the lifetime of the luminophore is expected to decrease to 100 ns if the RET efficiency is 90%. A decay time of 100 ns is still significantly longer than that seen with known red/NIR probes and also significantly longer than most autofluorescence, which typically decays in 10 ns. With a 10- μ s-decay-time donor, 90% transfer efficiency will result in a 1- μ s component in the acceptor decay. An important feature of a MLC tandem luminophore is an increased quantum yield. When energy transfer is rapid, most of the energy is transferred from the MLC to the acceptor. In this case, the quantum yield of the luminophore approaches the higher value of the directly excited acceptor rather than the lower value of the MLC.

We demonstrated the practical usefulness of these tandem luminophores using the covalently linked donor–acceptor (D–A) pairs shown in Scheme 1. These D–A pairs can be considered to be the probe or reagent, in the same manner that linked DNA pairs have been developed for DNA sequencing.^{32–33} Alternatively, this unique long-lifetime high-quantum-yield emission can be the result of protein or nucleic acid association reactions.

MATERIALS AND METHODS

The Texas Red iodoacetamide with a C5 linker was purchased from Molecular Probes, Inc. The $[\text{Ru}(\text{bpy})_2(\text{amino phenanthroline})]^{2+}$ was a gift from Dr. Jonathan Dattelbaum. The Ru MLC was synthesized following published procedures.^{18,19,24,25} It was converted into isothiocyanate by treating with 500 μL of thiophosgene in 1 mL of acetone for 3 h. Both the solvent and the thiophosgene were removed under a stream of nitrogen, and the isothiocyanate was used immediately.

The oligoproline peptides with a cysteine at the C-terminus were synthesized at the biopolymer facility of the University of Maryland School of Medicine, Baltimore. The crude peptides were purified by RP-HPLC on a C18 column using a gradient of 100% acetonitrile containing 0.05% TFA in 0.1% TFA. The molecular weights of the peptides were confirmed by mass spectroscopy.

The peptides were labeled first with the acceptor. Typically, a millimolar solution of the peptide in 0.2 M bicarbonate buffer, pH 8.5, was reacted with a 2-fold excess iodoacetamide for 6 h. The resulting peptide was purified from the free probe using a column of Sephadex G-15 running in 20% DMF solution. The labeled peptide was further purified by HPLC.

To prepare the double-labeled peptide, the acceptor-labeled peptide was further reacted with a 5-fold excess Ru isothiocyanate in 0.2 M bicarbonate, pH 9.0, for 6 h. The peptide was separated from the free probe by passing through a Sephadex G-15 column and was further purified on HPLC. To prepare the donor-only peptide, the sulfhydryl group was first blocked using a 5-fold excess iodoacetic acid at pH 8.5 for 1 h, and to the same reaction mixture, a 5-fold excess of the isothiocyanate was added, the pH was adjusted to 9, and it allowed to react for 6 h. The free dye was separated on a Sephadex G-15 column, and the donor-labeled peptide was purified by HPLC. The purified peptides were lyophilized and stored as water solutions at 4 °C.

The steady-state measurements were performed in an aqueous 5 mM hepes, 100 mM NaCl solution, pH 8. The measurements in propylene glycol were without buffer, with the propylene glycol at least 98%, the remainder being water. The peptide concentrations were $<2 \mu\text{M}$ for the steady-state measurements and about $10 \mu\text{M}$ for the time-resolved measurements. An aqueous solution of rhodamine B with a lifetime of 1.68 ns was used as the reference. The frequency-domain lifetime measurements were performed on a SLM instrument equipped with an LED emitting at 450 nm as a light source. The emission was observed through a 630/40-nm band-pass filter. The details of the instrumentation are published elsewhere.³⁴

THEORY

Resonance Energy Transfer

The theory and application of RET have been described in numerous reviews.^{35–37} Here, we discuss those aspects of RET that are needed to demonstrate the occurrence of a RET-enhanced quantum yield and the appearance of a long-lifetime component in the acceptor decay. The rate of energy transfer for a donor to an acceptor is given by

$$k_T = \frac{1}{\tau_D^0} \left(\frac{R_0}{r} \right)^6$$

(1)

where τ_D^0 is the donor lifetime in the absence of acceptor, r is the donor-to-acceptor distance, and R_0 is the Förster distance at which RET is 50% efficient. The value of R_0 can be accurately calculated from the spectral properties of the donor and acceptor.

Consider the donor–acceptor pair (Scheme 1). Assume the donor has a lifetime $\tau_D^0 = 1 \mu\text{s}$ and the acceptor, a lifetime of $\tau_A^0 = 1 \text{ ns}$ when directly excited. The efficiency of energy transfer is given by the ratio of the transfer rate to the total rate of donor deactivation, which is the reciprocal of the lifetime. Hence, the transfer efficiency (E) from the donor is given by

$$E = \frac{k_T}{k_T + \Gamma_D} = \left(\frac{k_T}{\lambda_D + k_D + k_T} \right)$$

(2)

where $\Gamma_D = (\tau_D^0)^{-1} = (\lambda_D + k_D)^{-1}$ is the decay rate of the donor in the absence of acceptor, and λ_D and k_D are the radiative and nonradiative decay rates, respectively (Scheme 2). The transfer efficiency (E) can be determined experimentally from the relative intensities of the donor in the absence (F_D) and presence (F_{DA}) of acceptor

$$E = 1 - \frac{F_{DA}}{F_D}$$

(3)

The transfer efficiency can also be determined from the donor decay times in the absence (τ_D^0) or presence (τ_D) of acceptors.

$$E = 1 - \frac{\tau_D}{\tau_D^0}$$

(4)

This expression is valid only when the donor decay is a single exponential. The decay time of the donor in the presence of acceptor is given by

$$\tau_D = 1/(k_T + \Gamma_D)$$

(5)

which is the reciprocal of the sum of the deactivation rates of the donor.

Steady-State Theory for Long-Wavelength Long-Lifetime High-Quantum-Yield Luminophores

The possibility of using rapid RET to improve the system quantum yield with low quantum yield donors can be seen from the equations that describe the donor (F_D) or acceptor (F_A) intensities. Consider the kinetic scheme shown in Scheme 2. The intensity of the donor and acceptor is proportional to the amount of light absorbed or the extinction coefficient (ϵ_D and ϵ_A) and the fraction of the absorbed light that is emitted. Hence, in the absence of RET

$$F_D^0 = \frac{\lambda_D \epsilon_D}{\lambda_D + k_D} = Q_D^0 \epsilon_D = \tau_D^0 \lambda_D \epsilon_D$$

(6)

$$F_A^0 = \frac{\lambda_A \epsilon_A}{\lambda_A + k_A} = Q_A^0 \epsilon_A = \tau_A^0 \lambda_A \epsilon_A$$

(7)

where ϵ_A and ϵ_D are the extinction coefficients at the wavelength used to excite the donor. The lifetimes of the unquenched donor and the directly excited acceptor are given by $(\tau_D^0)^{-1} = \lambda_D + k_D$ and $(\tau_A^0)^{-1} = \lambda_A + k_A$. The quantum yields of the donors or acceptors in the absence of energy transfer are given by the ratio of the emissive rates (λ_D or λ_A) to the sum of the rate process that depopulates the excited state ($\lambda_D + \lambda_D$) or ($\lambda_A + \lambda_A$). There is usually some acceptor emission, even in the absence of RET due to direct absorption (excitation) of the acceptor resulting from the nonzero value of ϵ_A . For clarity, we dropped the proportionality constant that should be on the right side of both eqs 6 and 7.

In the absence of RET, the total intensity (F_T^0) of the donor (F_D^0) and acceptor (F_A^0) is that due to direct excitation of both species

$$F_T^0 = F_D^0 + F_A^0 = \frac{\lambda_D \epsilon_D}{\lambda_D + k_D} + \frac{\lambda_A \epsilon_A}{\lambda_A + k_A} = Q_D^0 \epsilon_D + Q_A^0 \epsilon_A$$

(8)

where F_T^0 is the total emission in the absence of transfer. Now assume that RET occurs at a rate, k_T . The intensities of the donor and acceptor are given by

$$F_D = \frac{\lambda_D \epsilon_D}{\lambda_D + k_D + k_T} = Q_D \epsilon_D$$

(9)

$$F_A = \frac{\lambda_A \epsilon_A}{\lambda_A + k_A} + \frac{k_T \epsilon_D}{\lambda_D + k_D + k_T} \frac{\lambda_A}{\lambda_A + k_A}$$

(10)

The intensity or quantum yield of the donor, $Q_D = \lambda_D / (\lambda_D + k_D + k_T)$, is decreased by an additional rate k_T that depopulates the donor (eq 9). The intensity of the acceptor is increased by the transfer rate, k_T . The transfer efficiency term, $E = k_T / (\lambda_D + k_D + k_T)$, in eq 10 can be understood as the fraction of absorbed photons absorbed by the donor that are transferred to the acceptor. These transferred photons are emitted at a quantum yield, $Q_A = \lambda_A / (\lambda_A + k_A)$. The energy received from the donor is emitted at the quantum yield of the acceptor. The combined emission intensity of the donor and acceptor is given by

$$F_T = F_D + F_A = Q_D \epsilon_D + Q_A^0 (\epsilon_A + E \epsilon_D) = Q_D^0 \epsilon_D (1 - E) + Q_A^0 (\epsilon_A + E \epsilon_D)$$

(11)

It is instructive to consider the limits of very slow ($k_T \rightarrow 0$ and $E \rightarrow 0$) and very fast ($k_T \rightarrow \infty$) energy transfer. In the limit of no energy transfer, the total intensity becomes equal to that of a mixture of two noninteracting fluorophores (eq 8). In the limit of rapid transfer ($k_T \rightarrow \infty$ and $E \rightarrow 1$), the total intensity becomes

$$F_T = \frac{\lambda_A (\epsilon_A + \epsilon_D)}{\lambda_A + k_A} = Q_A (\epsilon_A + \epsilon_D)$$

(12)

This is an important result that indicates that the total intensity is proportional to both the sum of the extinction coefficients and the quantum yield of the acceptor. This occurs because the energy transfer can occur with an efficiency of 1, even if the donor quantum yield is low. If the rate of energy transfer is fast and if the acceptor absorbs weakly at the excitation wavelength ($\epsilon_A \ll \epsilon_D$) then

$$F_T = \frac{\lambda_A \epsilon_D}{\lambda_A + k_A} = Q_A \epsilon_D$$

(13)

This equation shows that with rapid energy transfer and no directly excited acceptor, the acceptor emission intensity is proportional to the amount of light absorbed by the donor and the quantum yield of the acceptor. The donor–acceptor pair becomes essentially a new “fluorophore” with an extinction coefficient ϵ_D and a quantum yield Q_A .

Kinetic Equations

It is informative to consider the time-dependent decays of the donor and acceptor and the total emission. These expressions are similar to those known for an excited-state reaction.^{38–41} In our case, the reverse transfer rate from A to D is zero (Scheme 2). Additionally, since both donor and acceptor are present all times, there is some direct excitation of the acceptor in addition to the acceptor that is excited by RET from the donor. The time-dependent changes in the donor and acceptor populations are given by

$$\frac{d[D]}{dt} = -(\Gamma_D + k_T)[D] + \epsilon_D L(t)$$

(14)

$$\frac{d[A]}{dt} = -\Gamma_A[A] + k_T[D] + \epsilon_A L(t)$$

(15)

where $L(t)$ is the excitation function. The square brackets are taken to indicate the excited-state population of each species. The time-dependent decays of the donor and acceptor are given by

$$I_D(t) = N_D^0 \exp[-(\Gamma_D + k_T)t]$$

(16)

$$I_A(t) = A \exp[-(\Gamma_D + k_T)t] + (N_A^0 - A) \exp[-\Gamma_A t]$$

(17)

where N_D^0 and N_A^0 are the number of excited donors and acceptor molecules at $t=0$. The preexponential factors in eqs 16 and 17 are proportional to $\epsilon_D L(t)$ and $\epsilon_A L(t)$, respectively, but are not shown. The factor A

$$A = \frac{N_D^0 k_T}{\Gamma_A - \Gamma_D - k_T} = \frac{-N_D^0 k_T}{\Gamma_A - \Gamma_D - k_T}$$

(18)

depends on the efficiency by which the acceptor is pumped by the donor. According to eq 16, the donor decay $I_D(t)$ is the usual decay rate of a donor having a transfer rate, k_T . The

acceptor decay contains a component with the lifetime of the acceptor, τ_A^0 , and a component with the lifetime of the quenched donor, τ_D .

Suppose the acceptor decay is very rapid; that is, the directly excited acceptor displays a short lifetime, $\tau_A \rightarrow 0$ or Γ_A is very large. Then the acceptor decay becomes

$$I_A(t) = A \exp[-(\Gamma_D + k_T)t]$$

(19)

This result shows that in the limit of a short acceptor lifetime, the acceptor emission resulting from energy transfer displays the same lifetime as the quenched donor. A similar result is shown if one assumes $\tau_D \ll \tau_A$ or $\Gamma_A \ll \Gamma_D$. In this case, the rightmost term in eq 17 decays rapidly to zero, relative to the donor decay, and the acceptor decay resulting from RET displays the same decay time as the donor. If there is no initially excited acceptor, $N_A^0 = 0$, the one obtains equal and opposite preexponential factors, and the acceptor decays according to

$$I_A(t) = A \exp[-(\Gamma_D + k_T)t] - A \exp[\Gamma_A t]$$

(20)

Simulations

We performed simulations to predict the spectral properties of the D–A pair for typical decay times and quantum yields. For these simulations, we modified eq 11 to use the normalized extinction coefficient ϵ_D' and ϵ_A'

$$Q_T = Q_A^0 \epsilon_D' (1 - E) + Q_A^0 (\epsilon_A' + E \epsilon_D')$$

(21)

where

$$\epsilon_D' = \epsilon_D / (\epsilon_D + \epsilon_A)$$

(22)

and

$$\epsilon'_A = \epsilon_A / (\epsilon_D + \epsilon_A)$$

(23)

Figure 1 shows the total quantum yield expected for three D–A pairs for various transfer efficiencies. We assumed the quantum yield of the acceptor was high, $Q_A^0 = 0.9$ (top), intermediate $Q_A^0 = 0.5$ (middle) and low $Q_A^0 = 0.1$ (lower panel). Because most acceptors will absorb at the donor excitation wavelength, we assumed the normalized extinction coefficient of the acceptor was $\epsilon'_A = \epsilon_A / (\epsilon_A + \epsilon_D) = 0.10$. As the transfer efficiency increases, the total quantum yield approaches that of the acceptor. If the acceptor quantum yield is low (lower panel), then energy transfer decreases the overall quantum yield. Importantly, if the quantum yield of the acceptor is high (upper panel), the overall quantum yield approaches that of the acceptor for high transfer efficiency.

We also simulated the intensity decays that are expected for the donor and acceptor in D–A pairs for various transfer efficiencies (Figure 2). The assumed decay times were $\tau_D^0 = 1000$ ns and $\tau_A^0 = 10$ ns. An important conclusion from these simulations is that the acceptor can display long decay times. For example, suppose the transfer efficiency is 33% (Figure 2, top panel). In this case the acceptor shows a decay time of $\tau = 667$ ns (Table 1). The transfer efficiency can be as high as 90.9% and the acceptor still display a 91 ns decay time. These simulations shows that usefully long decay times can be obtained even with high transfer efficiency.

RESULTS

We examined the emission spectra of Ru–(pro)₆-cys-TR (Scheme 1), which we will refer to as the (pro)₆ D–A pair. As a control for the donor alone (D), we used the structure shown in Scheme 1 with the sulfhydryl group blocked with iodoacetamide. For the acceptor (A), we used the structure shown in Scheme 1 without the covalently linked donor. Emission spectra of these three compounds are shown in Figure 3. These spectra were obtained using the same molar concentrations of D, A, and D–A. The overall intensity of the D–A pair is about 5-fold larger than the sum of the donor and acceptor alone. This result demonstrates that a tandem luminophore with a low quantum yield donor can display a higher quantum yield than either species alone.

Figure 4 shows the absorption and excitation spectra of D, A, and D–A. The absorption spectra of D–A was found to be essentially identical to the sum of the D-alone and A-alone absorption spectra (top). Contrasting results were found for the excitation spectra (Figure 4, bottom). In this case, the intensity of the long-wavelength emission with excitation at 450 nm is about 6-fold greater than that of the directly excited acceptor and about 20-fold larger

than the donor alone. This result also demonstrates the role of energy transfer in increasing the effective quantum yield of the donor.

The enhanced emission demonstrated in Figures 3 and 4 is determined by the relative extinction coefficients of the donor and acceptor at the excitation wavelength. The ratio of the donor to the absorption spectra is shown in the top panel of Figure 5. This ratio displays a maximum near 6 at 450 nm, which is near the peak of the donor absorption and the minimum of the acceptor absorption. The ratio of the excitation spectra shows the same trend, with a maximum near 450 nm (Figure 5, bottom). These results demonstrate that the enhancement at the acceptor emission is determined by the ratio of the light absorbed by each species.

We then questioned if the enhanced red emission with usefully long decay times could be obtained. This is an important consideration, because if the donor and acceptor are too close or if the rate of transfer is too fast, then the donor decay time will be shortened toward the nanosecond value characteristic of the directly excited acceptor. The frequency-domain intensity decay of D, A, and D–A are shown in Figure 6 (pro₆ linker) and Figure 7 (pro₇ linker). In both figures, the top panel represents results that were obtained in buffer, and in the lower panel are shown those obtained in propylene glycol. For ease of understanding, the frequency-domain data were used to reconstruct the time-dependent decays (Figure 8). In the absence of acceptor, the donor alone displays a mostly single exponential decay with a decay time of 515 ns (top panel, Figures 6 and 7). The donor decay time is longer in propylene glycol (bottom panel, Figures 6 and 7), near 820 ns. The decay time of the directly excited acceptor is much shorter and is near 4 ns in either solvent.

The D–A pairs measured at the acceptor emission wavelength display a more complex intensity decay, as can be seen from the frequency responses for D–pro₆-A (Figure 6) or D–pro₈-A (Figure 7). One notices that the sensitized acceptor emission in both D–A pairs displays a longer decay time, as seen from the shift to lower frequency. When the D–A pairs are compared, the sensitized emission from D–pro₈-A is longer-lived than that from D–pro₆-A. The intensity decay parameters obtained from multicomponent analysis are summarized in Table 2. For a D–A pair at a single distance, one expects a single decay time for the donor. The heterogeneous decays of the D–A pairs are the result of a range of D–A distances because of the flexibility of the linkers, especially the linker to Texas Red. There are 12 chemical bonds between the last proline and Texas Red; however, it is possible to synthesize an acceptor with a shorter linker, which should result in a more homogeneous decay. Nonetheless, the D–pro₆-A displays a long decay time near 22 ns in water and 55 ns in propylene glycol, and we observe times of 50 ns (buffer) and 130 ns (propylene glycol) in the case of D–pro₈-A. The longer lifetimes in for D–pro₈-A are expected, because the D and A are separated by a larger distance. We assigned these longer-lived components as due to the acceptors that are being excited by RET from the excited donor population. In the case of D–pro₆-A, the sensitized acceptor lifetime suggests a RET efficiency greater than 95%, which is corroborated by the steady-state intensity results. It is also clear from the results obtained with D–pro₈-A that long decay times exceeding 100 ns can be obtained using such tandem luminophores.

DISCUSSION

Many reports have appeared on the use of the acceptor emission to quantify the RET transfer efficiency. These include numerous primary reports and review articles, so the use of the acceptor emission to measure the transfer efficiency is not new.^{42–45} In addition, Selvin and co-workers have already noted the usefulness of measuring the long time acceptor emission with lanthanide donors to selectively detect D–A pairs⁴⁶ and to modify the long decay time of the acceptor using spacers.^{47–48} Additionally, covalently linked donors and acceptors, both with short decay times, have been developed for use in DNA sequencing^{32,33} and as high-affinity dyes that bind noncovalently to DNA.^{49–50} The novelty in the present report is recognition that the effective quantum yield of the luminophore could be increased by rapid RET. Such an increase in effective quantum yield has not been important in the biochemical uses of RET,^{42–50} because most organic donors have good quantum yields. The increased effective quantum yield of the donor has not been important for RET with the lanthanides, because transfer from the organic chelates to the lanthanides is efficient, and the shielded lanthanide donors often display quantum yields near unity. The value of the RET-enhanced quantum yield becomes apparent only because of the development of the long-lifetime MLC probes and their low quantum yield. In retrospect, the possibility of increasing the effective quantum yield of the donor was “known” by the enhancement of lanthanide emission when bound to essentially nonluminescent DNA or nucleotides.^{51–53} However, to the best of our knowledge, the practical utility of the RET-enhanced effective quantum yield with low quantum yield donors has not been previously reported.

From eqs 12 and 13, it is obvious that the effective quantum yield of such probes will be governed by the molar extinction of the donor and the quantum yield of the acceptor. The Ru MLCs have significantly lower molar extinctions ($<20\,000\text{ M}^{-1}\text{ cm}^{-1}$) when compared to fluorescein-like organic fluorophores with molar extinctions approaching $100\,000\text{ M}^{-1}\text{ cm}^{-1}$. However, there are examples of Ru MLCs that are sensitized with organic fluorophores and have molar extinctions comparable to those seen in fluorescein-like molecules (ref 20 and references therein). Another, and even more important, fact is that the longer lifetimes of such tandem probes will allow off-gating of the nanosecond autofluorescence. The use of gating with sensitized lanthanide emission has been shown to provide high sensitivity detection in biological samples.^{54–56} We believe similar sensitivity will be available to these probes when combined with appropriate gating.

We feel that our approach to tandem luminophores can be rationally used to obtain the desired spectral properties. RET is a highly predictable phenomena, and the long acceptor decay time could be increased by a longer spacer. Additionally, less spectral overlap of the D and A could be obtained using shorter-wavelength rhenium MLC donors or longer-wavelength acceptors. These tandem luminophores can be prepared in conjugatable forms and used as a single reagent. And finally, this concept can be applied to the measurement of protein or DNA association reactions in which the donor and acceptor are present in separate molecules.

ACKNOWLEDGMENT

This work was supported by the NIH, RR-08119. The authors thank Dr. Jonathan Dattelbaum for providing the ruthenium metal–ligand complexes.

References

- (1). Thompson RB In Topics in Fluorescence Spectroscopy; Lakowicz JR, Ed.; Plenum Press: New York, 1994; Vol.4, pp 151–222.
- (2). Daehne S; Resch-Genger U; Wolfbeis OS In Near-Infrared Dyes for High Technology Applications, Daehne S, Ed.; Kluwer Academic Publishers: Netherlands, 1998, p 458.
- (3). Southwick PL; Ernst LA; Tauriello EW; Parker SR; Mujumdar RB; Mujumdar SW; Clever HA; Waggoner AS Cytometry 1990, 11, 418–430. [PubMed: 2340776]
- (4). Rahavendran SV; Karnes HT J. Pharm. Biomed Anal 1996, 15, 83–98. [PubMed: 8895079]
- (5). Rahavendran SV; Karnes HT Anal. Chem 1996, 68, 3763–3768. [PubMed: 21619248]
- (6). Kessler MA; Wolfbeis OS Anal. Biochem 1992, 200, 254–259. [PubMed: 1378702]
- (7). Middendorf L; Amen J; Bruce R; Draney D; DeGraff D; Gewecke J; Grone D; Humphrey P; Little G; Lugade A; Narayanan N; Oommen A; Osterman H; Peterson R; Rada J; Raghavachari R; Roemer S In Near-Infrared Dyes for High Technology Applications, Daehne S, Ed.; Kluwer Academic Publishers: Netherlands, 1998; pp 21–54.
- (8). Flanagan JH; Romero SE; Legendre BL; Hammer RP; Soper A SPIE Proc. 1997, 2980, 328–337.
- (9). Owens CV; Davidson YY; Kar S; Soper SA Anal. Chem 1997, 69, 1256–1261.
- (10). Abugo OO; Nair R; Lakowicz JR Anal. Biochem 2000, 279, 142–150. [PubMed: 10706783]
- (11). Dorshow RB; Bugaj JE; Burleigh BD; Duncan JR; Johnson MA; Jones WB J. Biomed. Optics 1998, 3, 340–345.
- (12). Kanda M; Niwa S Appl. Optics 1992, 31, 6668–6675.
- (13). Bollinger A; Saesseli B; Hoffmann U; Franzeck UK Circulation 1991, 83, 546–551. [PubMed: 1991372]
- (14). Strickler SJ; Berg RA J. Chem. Phys 1962, 37, 814–822.
- (15). Nikolaitchik AV; Korth O; Rodgers MA J. J. Phys. Chem. A 1999, 103, 7587–7596.
- (16). del Ray B; Keller U; Torres T; Rojo G; Aguillo-Lopez F; Nonell S; Marti C; Brasselet S; Ledoux I; Zyss J J. Am. Chem. Soc 1998, 120, 12808–12817.
- (17). Howe L; Sucheta A; Einarsdottir O; Zhang JZ Photochem. Photobiol 1999, 69, 617–623. [PubMed: 10377999]
- (18). Kalayanasundaram K Photochemistry of Polypyridine and Porphyrin Complexes; Academic Press: New York, 1992.
- (19). Juris A; Balzani V; Barigelletti F; Campagna S; Belser P; Von Zelewsky A Coord. Chem. Rev 1988, 84, 85–277.
- (20). Tyson DS; Castellano FN J. Phys. Chem. A 1999, 103, 10955–10960.
- (21). Stiffens DJ; Aarnts MP; Rossenaar BD; Vlcek A Pure Appl. Chem 1997, 69, 831–835.
- (22). Simon JA; Curry SL; Schmehl RH; Schatz TR; Piotrowiak P; Jin X; Thummel RP J. Am. Chem. Soc 1997, 119, 11012–11022.
- (23). Harriman A; Hissler M; Khatyr A; Ziessel R Chem. Commun 1999, 735–736.
- (24). Demas JN; DeGraff BA Anal. Chem 1991, 63, 829A–837A.
- (25). Demas JN; DeGraff BA In Topics in Fluorescence Spectroscopy; Lakowicz JR, Ed.; Plenum Press: New York, 1994; Vol. 4, pp 71–107.
- (26). Terpetschnig E; Szmecinski H; Malak H; Lakowicz JR Biophys.J 1995, 68, 342–350. [PubMed: 7711260]
- (27). Szmecinski H; Terpetschnig E; Lakowicz JR Biophys. Chem 1996, 62, 109–120. [PubMed: 8962474]
- (28). Guo X-Q; Castellano FN; Li L; Lakowicz JR Anal. Chem 1998, 70, 632–637. [PubMed: 9470490]

- (29). Murtaza Z; Lakowicz JR SPIE Proc. 1999, 3602, 309–315.
- (30). Grigg R; Norbert WDJ J. Chem. Soc. Chem. Commun 1992, 1300–1302.
- (31). Lippitsch ME; Wolfbeis OS Anal. Chim 1988, 205, 1–6.
- (32). Ju J; Ruan C; Fuller CW; Glazer AN; Mathies RA Proc. Natl. Acad. Sci. U.S.A 1995, 92, 4347–4351. [PubMed: 7753809]
- (33). Ju J; Glazer AN; Mathies RA Nat. Med 1996, 2, 246–249. [PubMed: 8574973]
- (34). Herman P; Maliwal BP; Lin H-J; Lakowicz JR J. Microsc 2001, 203, 176–181. [PubMed: 11489073]
- (35). Stryer L Annu. Rev. Biochem 1978, 47, 819–846. [PubMed: 354506]
- (36). Clegg RM In Fluorescence Imaging Spectroscopy and Microscopy, Wang XF, Herman B, Eds.; John Wiley & Sons: New York, 1966; pp 179–252.
- (37). Lakowicz JR Principles of Fluorescence Spectroscopy, 2nd ed.; Kluwer Academic/Plenum Publishers: New York, 1999, Chapters 13–15.
- (38). Laws JR; Brand LJ Phys. Chem 1979, 83, 795–802.
- (39). Gafni A; Brand L Chem. Phys. Lett 1978, 58, 346–350.
- (40). Lakowicz JR; Balter A Biophys. Chem 1982, 16, 99–115. [PubMed: 7139052]
- (41). Lakowicz JR; Balter A Biophys. Chem 1982, 16, 117–132. [PubMed: 7139044]
- (42). Cheung HC In Topics in Fluorescence Spectroscopy, Lakowicz JR, Ed.; Plenum Press: New York, 1991; Vol. 2, pp 127–176.
- (43). Clegg RM Proc. Natl. Acad. Sci. U.S.A 1992, 211, 353–388.
- (44). Clegg RM; Murchie AI; Zechel A; Lilley DM Proc. Natl. Acad. Sci. U.S.A 1993, 90, 2994–2998. [PubMed: 8464916]
- (45). Root DD Proc. Natl. Acad. Sci. U.S.A 1997, 94, 5685–5690. [PubMed: 9159133]
- (46). Selvin PR IEEE J. Sel. Top. Quantum Electron 1996, 2, 1077–1087.
- (47). Chen J; Selvin PR J. Am. Chem. Soc 2000, 122, 657–660.
- (48). Selvin PR; Hearst JE Proc. Natl. Acad. Sci. U.S.A 1994, 91, 10024–10028. [PubMed: 7937831]
- (49). Benson SC; Mathies RA; Glazer AN Nucleic Acids Res. 1993, 21, 5720–5726. [PubMed: 8284220]
- (50). Benson SC; Zeng Z; Glazer AN Anal. Biochem 1995, 231, 247–255. [PubMed: 8678308]
- (51). Klakamp SL; Horrocks W DeW. J. Inorg. Biochem 1992, 46, 175–192. [PubMed: 1517730]
- (52). Klakamp SL; Horrocks W DeW. J. Inorg. Biochem 1992, 46, 193–205. [PubMed: 1517731]
- (53). Fu PKL; Turro CJ Am. Chem. Soc 1999, 121, 1–7.
- (54). Hemmila I; Mikkala V-M; Takalo HJ Alloys Compd. 1997, 249, 158–162.
- (55). Hemmila IJ Alloys Compd. 1995, 225, 480–485.
- (56). Yuan J; Wang G; Majima K; Matsumoto K Anal. Chem 2001, 73, 1869–1876. [PubMed: 11338604]

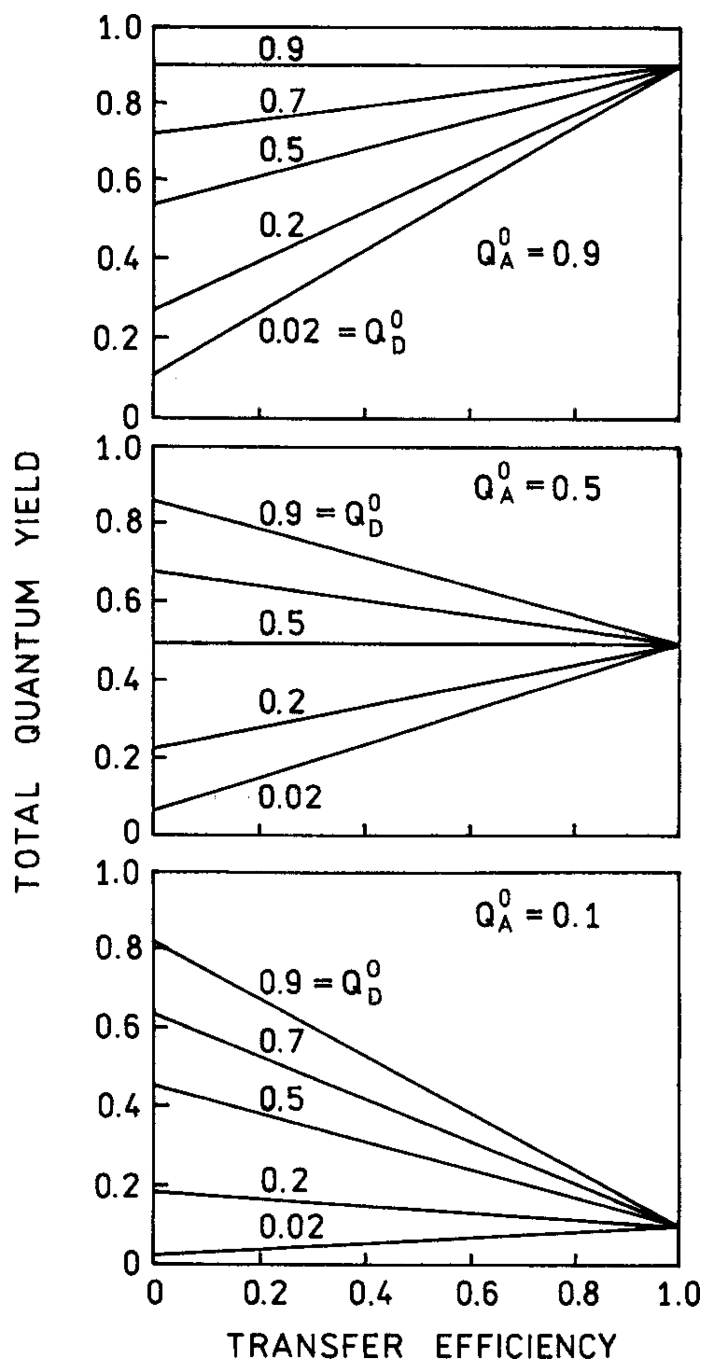


Figure 1.
Effect of energy transfer efficiency on the total quantum yield.

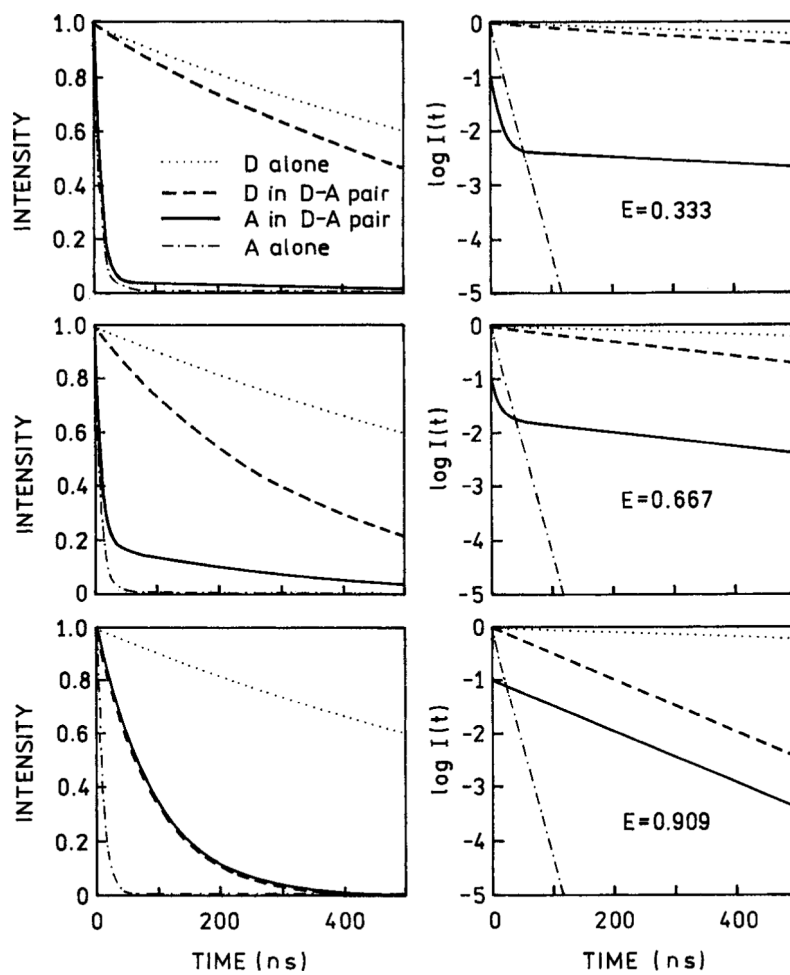


Figure 2. Simulated time-dependent decays of the donor and acceptor, each alone and in a D–A pair. For these simulations, $\tau_D^0 = 1000$ ns, and $\tau_A^0 = 10$ ns.

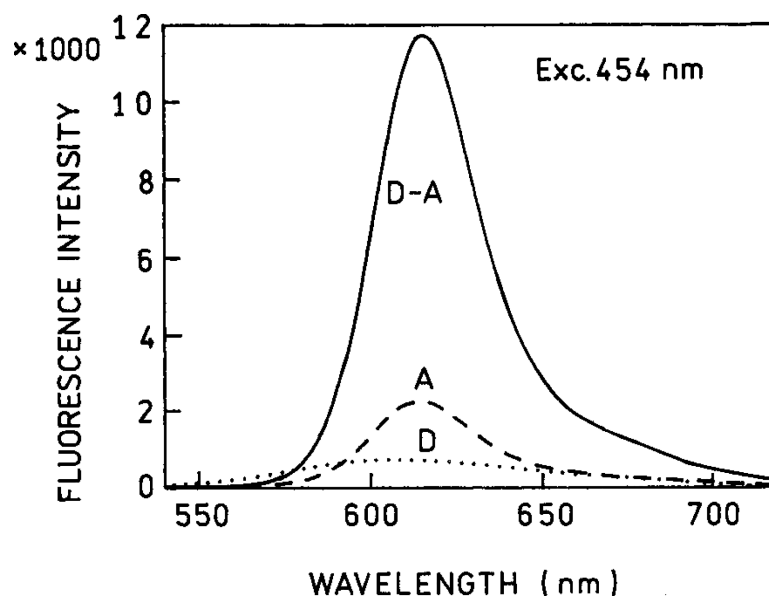


Figure 3. Emission spectra of the Ru-(pro)₆ donor (D) the TR acceptor (A) and the covalently linked pair (D-A) in aqueous buffer.

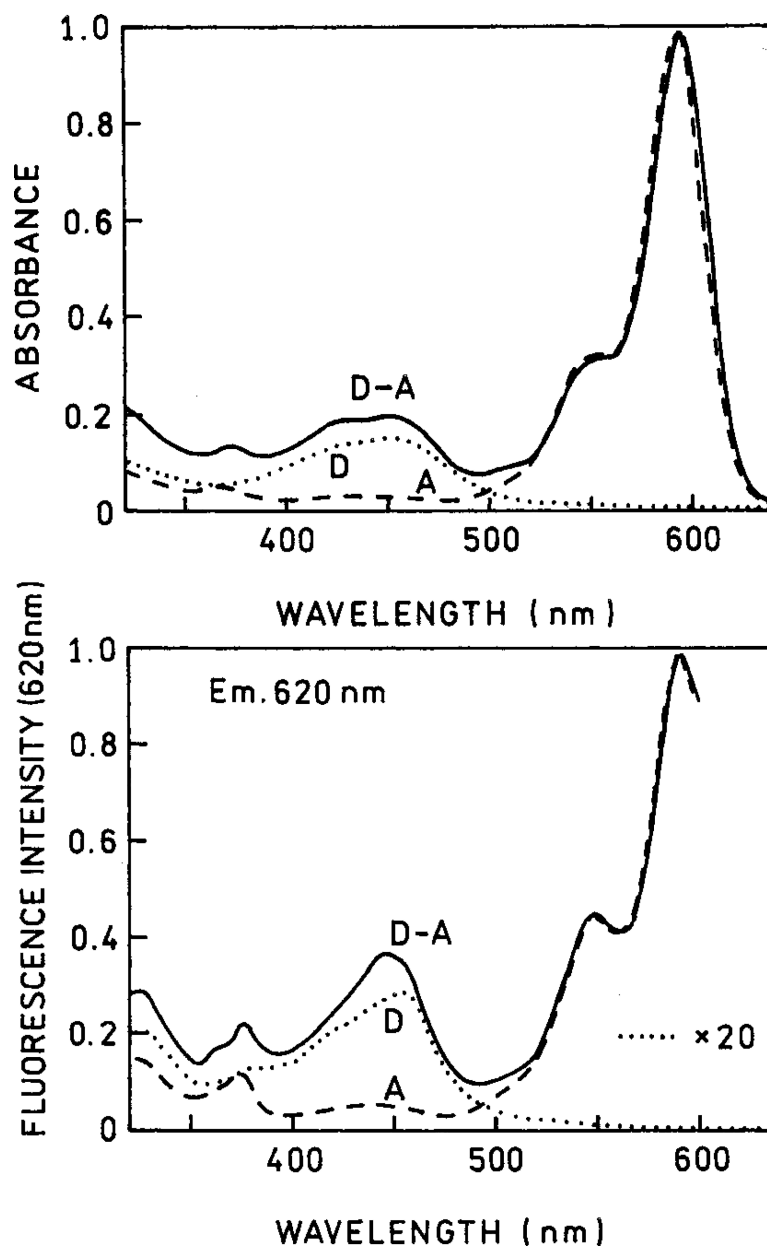


Figure 4. Absorption (top) and excitation (bottom) spectra of Ru-(pro)₆(D), TR(A), and Ru-(pro)₆-TR (D-A) in aqueous buffer.

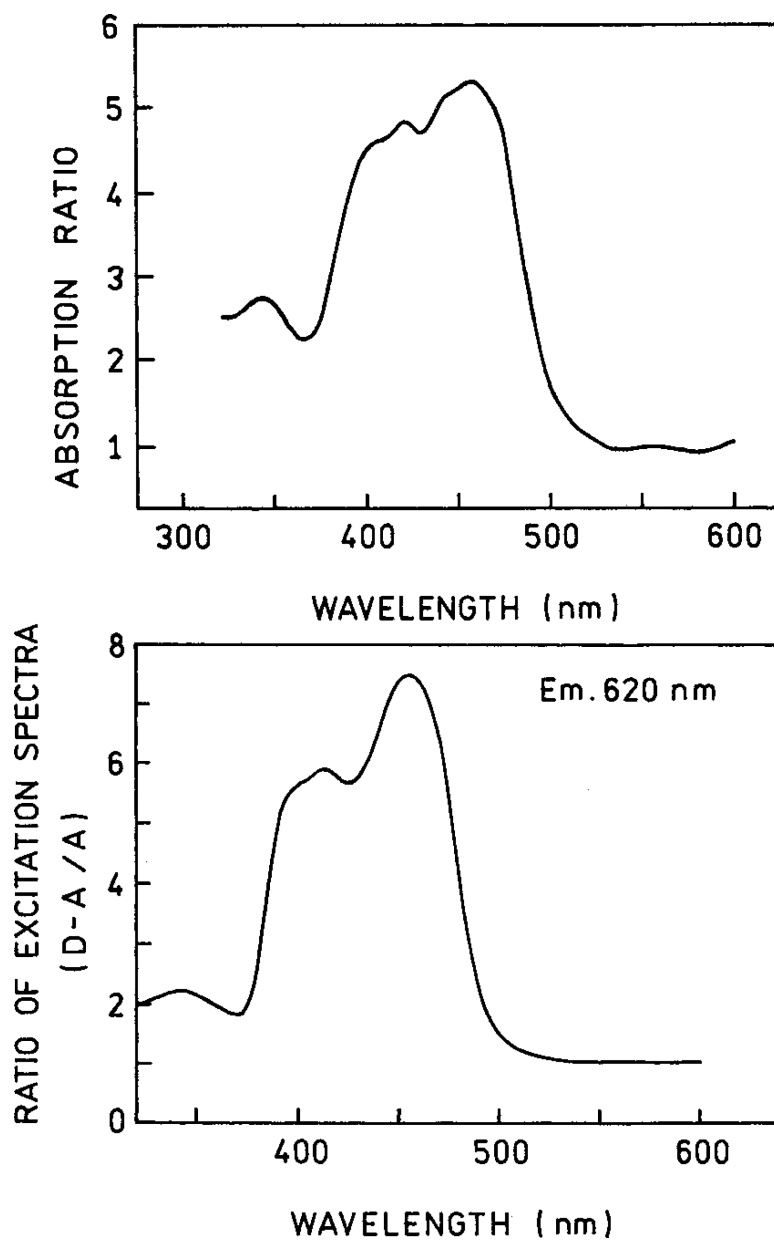


Figure 5. Ratio of the absorption spectra (top) and emission spectra (bottom) of the D–A pair divided by that of the acceptor in aqueous buffer.

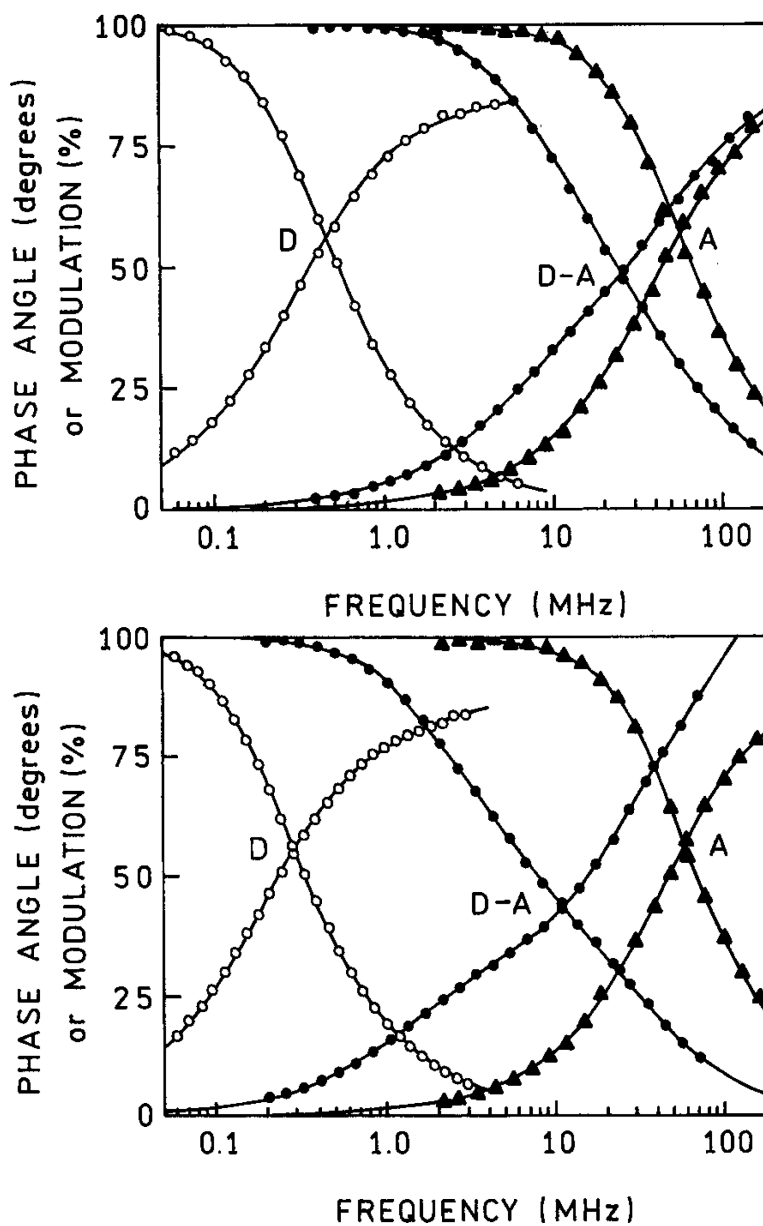


Figure 6. Frequency domain intensity decays of the donor alone (D), acceptor alone (A), and the covalently linked D-pro₆-A pair in aqueous buffer (top) and in propylene glycol (bottom).

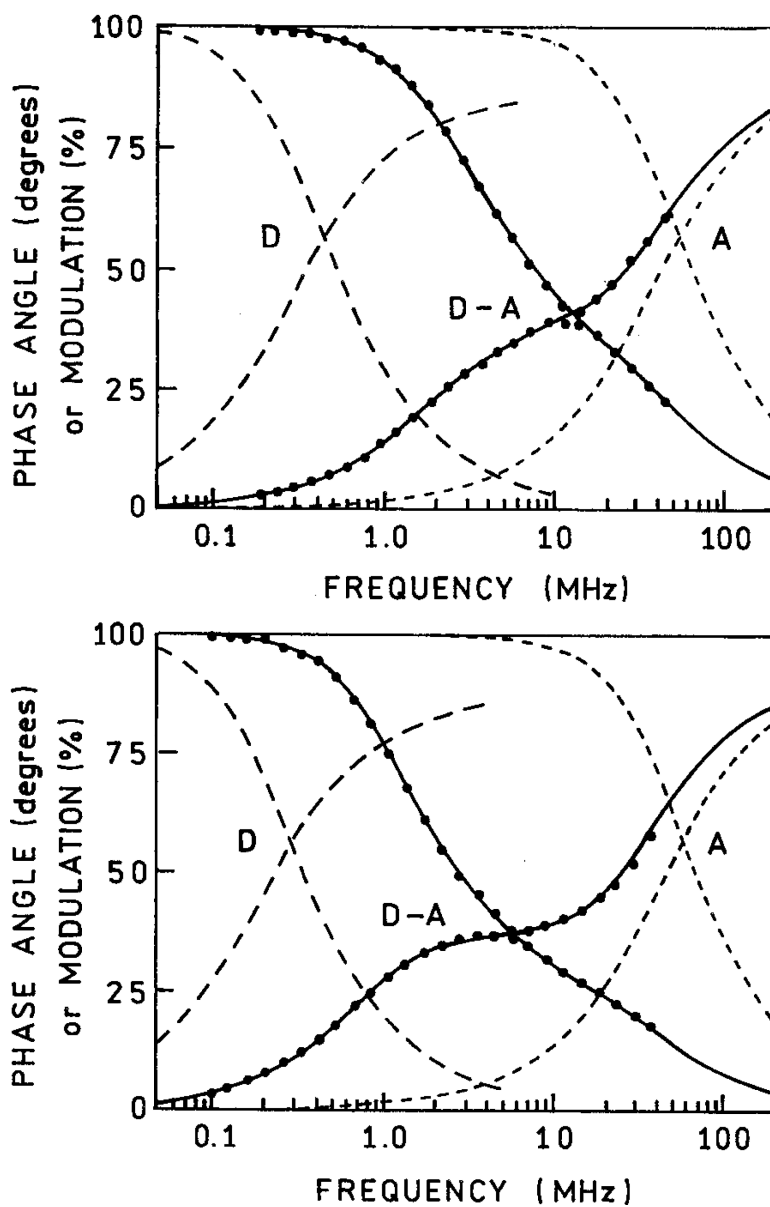


Figure 7. Frequency domain intensity decays of the donor alone (D), acceptor alone (A), and the covalently linked D-prog-cys-A pair in the aqueous buffer (top) and in propylene glycol (bottom).

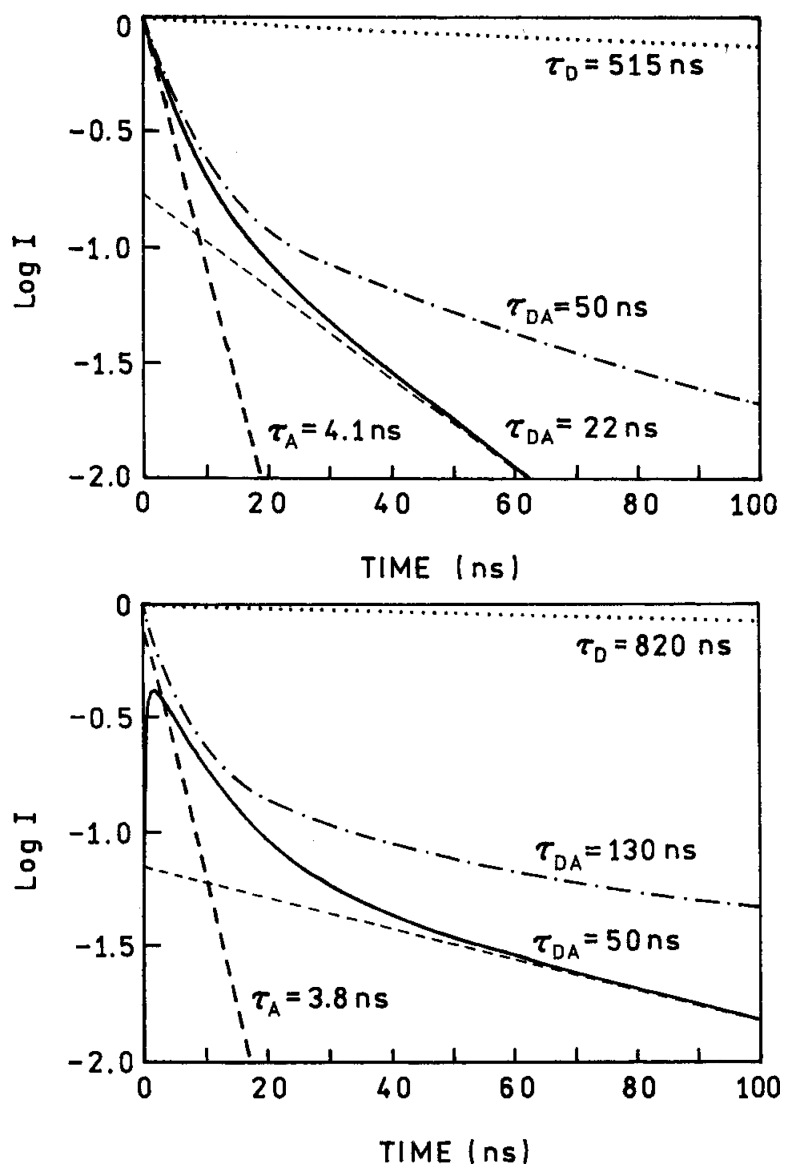
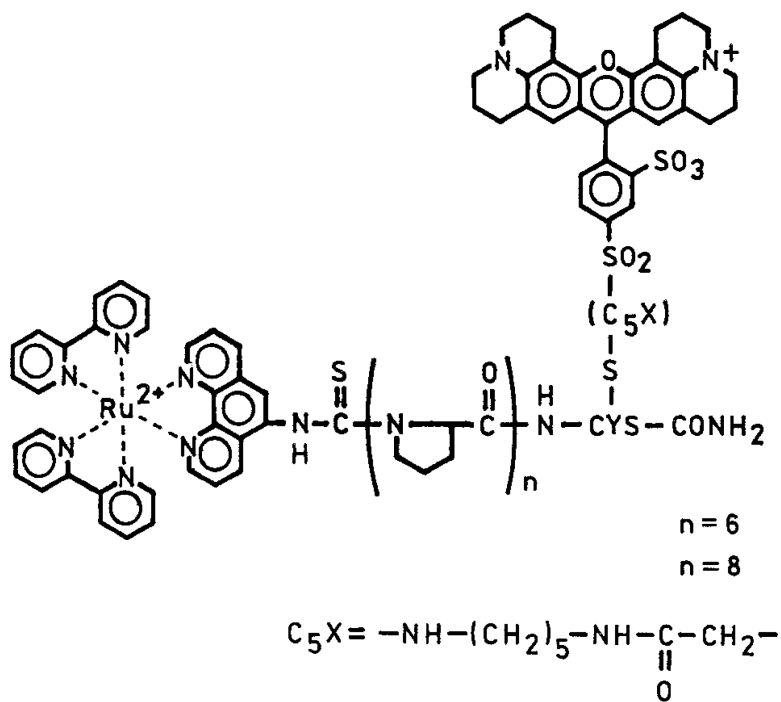


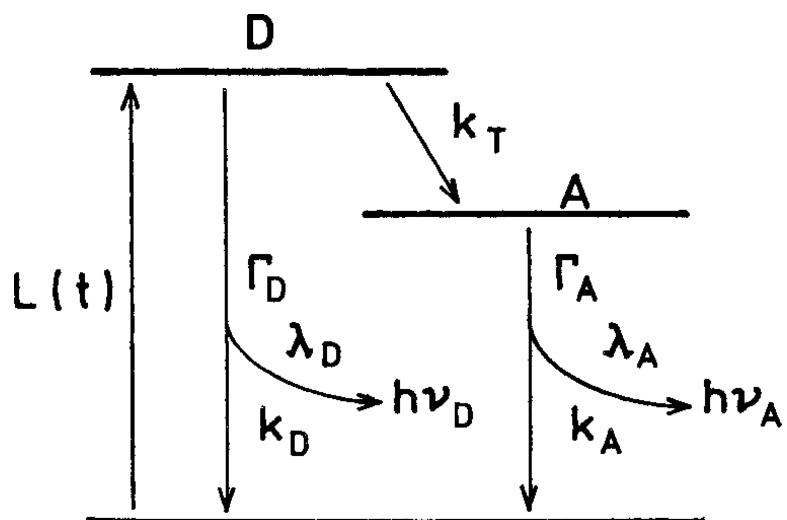
Figure 8. Reconstructed time-domain intensity decays of the donor alone (D), acceptor alone (A), and the covalently linked pair (D-A) in water (top) and in propylene glycol (bottom). The solid line, τ_{DA} , is for D-prog₆-A and the dashed-dotted (-•-•-) line, τ_{DA} , is for D-prog₈-A.



Ru-(pro)_n-cys-TR

Scheme 1. Chemical Structure of a Ru MLC Covalently Linked to Texas Red (D-A)^a

^a The donor-alone control had the sulfhydryl group blocked with iodoacetamide. The acceptor alone was the peptide without the MLC group.



Scheme 2. Jablonski Diagram for an Irreversible Excited-State Process

Table 1.Expected Lifetimes and Total Quantum Yields for D–A Pairs^a

transfer efficiency E	acceptor fluorescence τ_1 ns	lifetimes τ_2 ns	total quantum yield of the system $Q_T = Q_D + Q_A$
0	10		0.108
0.091	10	909	0.180
0.333	10	667	0.372
0.500	10	500	0.504
0.667	10	333	0.636
0.833	10	167	0.768
0.909	10	91	0.829
0.950	10	48	0.860
0.980	10	20	0.884

^a $\tau_D^0 = 1000$ ns, $\tau_A^0 = 10$ ns, $Q_D^0 = 0.02$, $Q_A^0 = 0.90$. For these calculations, we assumed the extinction coefficient of the donor is 9-fold larger than that of the acceptor at the excitation wavelength.

Table 2.Multiexponential Intensity Decay Analysis for the Donor, Acceptor, and D–A Pairs Shown in Scheme 1^a

solvent/compd	Q	α_i^b	f_i	τ_i	χ_R^2
Water					
D-pro ₆	0.0333	0.099	0.009	41.2	1.45 ^c
		0.901	0.991	516.7	
pro ₆ -A	0.360	1.0	1.0	4.0	1.26
D-pro ₆ -A	0.33	0.469	0.198	3.5	0.82
		0.353	0.304	7.0	
		0.178	0.458	22.7	
D-pro ₈ -A		0.784	0.287	4.4	0.87
		0.137	0.252	22.3	
		0.079	0.461	71.1	
Propylene Glycol					
D-pro ₆		0.125	0.014	79.4	0.98
		0.875	0.986	785	
pro ₆ -A		1.0	1.0	4.1	2.36
D-pro ₆ -A		0.803	0.363	7.9	
		0.178	0.245	33.4	
		0.069	0.392	99.5	0.51
D-pro ₈ -A		0.839	0.225	5.1	1.3
		0.089	0.170	36.3	
		0.072	0.604	157.8	

^aExcitation was at 455 nm using a blue-light-emitting diode. The emission was measured at 630 nm with a 25-nm band-pass.^bThe decays were analyzed internally at the multiexponential model, $I(t) = \sum \alpha_i \exp(-t/\tau_i)$, $f_i = \alpha_i \tau_i / \sum \alpha_j \tau_j$.^c $\delta p = 0.3^\circ$ and $\delta m = 0.003$.